Power scaling of continuous-wave adaptive gain-grating laser resonators

Jason M Hendricks, David I Hillier, Steve J Barrington,

David P Shepherd, Robert W Eason

Optoelectronics Research Centre,

University of Southampton,

Southampton,

SO17 1BJ,

UK.

Michael J Damzen, Ara Minassian, Benjamin Thompson

The Blackett Laboratory

Imperial College,

London,

SW7 2BW

UK.

Key-words: Phase conjugation, Gain-grating, Diode-pumped, thermal distortion.

PACS: 42.65.Hw, 42.55.Xi, 42.25.Hz, 42.40.Pa

Abstract

We demonstrate a power-scaling strategy in a continuous-wave adaptive phase-conjugate oscillator power amplifier (PCO-PA) system that actively corrects, via phase-conjugation, for thermally induced phase-distortions introduced by a power-amplifier (PA) placed in the output arm of the phase conjugate oscillator (PCO). Phase-conjugation is achieved by saturable gain four-wave mixing in a PCO Nd:YVO_4 amplifier. Single-longitudinal mode phase-conjugate (PC) outputs of almost 11.5 W with an $M_x^2 = 1.4$, $M_y^2 = 1.2$ have so far been achieved with a PCO operating at 6 W PC output, a power gain of two through the PA. The saturable gain four-wave mixing that takes place in the PCO-PA system has been modelled and the results can be used to predict how best to proceed with further increasing the PC output power from such a system.

Introduction

Diode pumping of solid-state lasers has been the subject of intense research in the last few years as a way of producing high-power, high brightness outputs in a relatively cheap, compact device. The continuous-wave power output from commercial diode bars can now exceed 60 watts whilst the stacking of several such bars can produce devices capable of delivering up to 600 W CW [1]. The major drawback of pumping a crystal with such high pump power densities is that more heat energy is deposited into the crystal primarily through quantum defect heating (24% of the pump power absorbed in a Nd:YVO_4 crystal is converted to heat) [2] and secondly through competing spectroscopic effects such as energy transfer upconversion (ETU) which adds to the thermal loading of the crystal through the subsequent non-radiative decays [3]. This heating effect is detrimental to the lasing process in several ways. First of all, the refractive index of the crystal is a function of its temperature, so as more heat is deposited the local change in refractive index can cause aberrations in the transverse-mode of the cavity affecting the laser stability. Secondly, the temperature rise in the crystal induces stress to the lattice which can manifest itself as stress-induced birefringence, the physical bulging of the end face causing a lensing effect or more catastrophically damage or fracture of the crystal.

Much ongoing work now concerns itself with scaling the power from diode-pumped solid-state lasers whilst simultaneously reducing the thermal effects to maintain near diffraction-limited output at a high power and hence high brightness [4]. One avenue that has seen much interest is the use of phase-conjugation to correct for the phase-distortions within the amplifier. We have recently reported a laser cavity operating on

a single-longitudinal TEM_{00} mode that could actively adapt itself to maintain single-mode spatial operation even when severe passive phase-aberrations were introduced inside the resonator [5]. The operation of the resonator depended on dynamic gain-gratings written via spatial-hole burning in the population-inverted region of the pumped crystal [6]. Successful correction of the intracavity distortions occurred when the backwards-travelling mode of the ring-resonator was the phase-conjugate of the forward travelling distorted mode.

In this paper, we demonstrate for the first time power scaling of a continuous-wave adaptive laser resonator based on the gain-grating technique. We show that the addition of a Nd:YVO_4 power-amplifier into our previously demonstrated resonator can almost double its output from ~6 W up to ~11.5 W whilst still maintaining single longitudinal and transverse mode operation. We also present a model of the interaction geometry in the PCO-PA system and address the question of further increasing the available power output.

Operation of the PCO-PA

Figure 1 shows a schematic of the adaptive resonator with an additional power amplifier in the output arm. A 300 mW 1064 nm Nd:YAG seed-laser, used to define the transverse PC mode of the system, is launched into the four-wave mixing (FWM) amplifier where it is amplified and sent around the resonator so that it overlaps with itself back inside the FWM amplifier. The interference pattern produced when the two beams overlap modulates the gain of the FWM amplifier to produce a volume gain-grating, which encodes any phase distortion experienced by the seed laser as it passes around the loop, including distortions, such as thermal lensing, from the gain region itself. In the clockwise direction (see figure 1) a phase-conjugate lasing mode can build up from any coherent amplified-spontaneous emission that is scattered from the volume gain-grating formed. In this way the phase-conjugate mode is automatically Bragg matched to the grating. The first-order diffraction from the grating then oscillates in the clockwise direction, so that the loop is closed by the presence of this gain-grating. The zero order from the grating (the undiffracted part of the phase-conjugate mode) travels back along the original seed beam direction, through the power-amplifier, to become the output, all the time remaining the phase-conjugate of the seed laser and hence ensuring a high spatial quality beam. The efficiency of operation of the resonator can be increased by the addition of a non-reciprocal transmission element (NRTE) consisting of a Faraday rotator and a half-wave plate between two vertical polarisers. In the anti-clockwise direction this allows reduction of the intensity of the amplified seed laser so that the intensities of the two intersecting beams that write the gain-grating can be matched to produce the optimum

modulation in the interference pattern for highest diffraction efficiency of the gain-grating. In the clockwise direction the NRTE has near-unity transmission.

The FWM amplifier used in the PC resonator is a transversely diode-pumped 1.1 atm% neodymium doped yttrium ortho-vanadate ($Nd:YVO_4$) a-cut slab with dimensions 20x5x3 mm [7]. The 5x3mm a-faces were AR coated for 1064 nm and the b-faces were AR coated for the diode-pump wavelength of 808 nm. The pump source for the FWM amplifier was a 60 W CW diode-bar, collimated in the fast direction by an aspheric cylindrical lens pre-mounted on the diode-bar and focussed into the crystal by a second cylindrical lens of focal length f = 6.35 mm. The diode output was TM polarised ensuring that the pump light was parallel with the c-axis of the crystal which lead to maximum pump absorption ($\alpha = 30\ cm^{-1}$). The reflection of all resonator beams (the FP, BP and S) from the pumped b-face of the crystal ensured that the region of highest gain (that nearest the pump face) was accessed and that the gain seen by the beams was nearly uniform across their widths [8]. The beams were focussed into the gain regions using spherical focussing lenses of focal length f = 100 mm giving a calculated focussed spot size in the gain region of ~40 μm.

The power-amplifier in the output arm of the adaptive resonator used the same bounce geometry as the FWM amplifier (reflection from b-face), but had the following differences. The pump source was a TE polarised 34 W diode-laser whose polarisation was rotated to be parallel with the crystal c-axis by using a half-wave plate. The pump-beam was focussed into the crystal using a 12.7mm cylindrical lens and the dimensions of the $Nd:YVO_4$ crystal were 20x5x1 mm. The two a-faces (5x1 mm) had a ~2° wedge to suppress parasitic lasing inside the crystal.

Lasing results for the PCO-PA

Figure 2 shows the PC output power from the adaptive laser resonator with the power-amplifier in the arm as a function of the seed laser input power. The first curve (diamonds) shows the output when the power-amplifier had a small-signal single-pass (SSSP) gain of 1 (amplifier un-pumped). As the seed input power is increased from a low value the PC output power also increases. In this region, the saturation depth of the gain grating in the FWM amplifier is increasing and so its diffraction efficiency increases with increasing input power. The maximum output of ~6 W from the resonator occurred at an input power of ~20 mW. Beyond this value the PC output begins to fall as the gain is oversaturated.

With the amplifier turned on, its gain was varied by defocusing the cylindrical lens used to focus the light from the pump diode into the crystal. In this set-up the PCO was left in exactly the same configuration as for the first set of results (diamonds). In this way we could see how, for a set configuration of the PCO, and hence a known input-output curve, the PA affected the results for the combined PCO-PA. It is important to note that keeping the PCO constant whilst varying the PA will not necessarily produce the maximum power output as it is likely that some optimum distribution of gain will occur between the FWM amplifier and the PA. The existence of an optimised gain distribution is explored later in the theory section.

The second curve in figure 2 (triangles) show the PC output when the power-amplifier has a SSSP gain of ~5. Here the peak output occurs for around 10 mW seed laser input giving a power output of the PCO-PA of ~8 W. The third curve (squares) shows

the PC output when the PA has a SSSP gain of ~10. The seed input for maximum output occurs at ~4.3 mW giving a total power output from the PCO-PA of 11.4 W.

To examine the effect of varying the gain of the PA on the PCO (which was not changed throughout the experiment) the power within the PCO was measured in the clockwise direction in figure 1 by placing a 4% reflectivity wedge at point A and sampling a small amount of circulating power. Figure 3 shows the measured intracavity-flux at this point as a function of the seed-input power. It can be seen that for all three different SSSP gains of the PA the shape of the curves remain fairly constant but are progressively shifted towards lower seed input powers as the PA gain is increased. These results would suggest that for any given configuration of the PCO i.e. SSSP gain of the FWM amplifier, angle of the beams, NRTE transmission etc, the input-output curves for that PCO remain essentially constant regardless of the gain of the PA in the output arm.

Figure 4(a) shows the spatial output from the PCO when the PA pumping is turned off (SSSP gain = 1). The output power is ~6 W and it operates on a near diffraction limited mode. The beam is elliptical in geometry due to the asymmetry of the gain region in the FWM amplifier (a $1/e^2$ absorption depth of around 300 μm for $Nd:YVO_4$ and a $1/e^2$ height of ~40 μm for the diode focussed into the crystal). The output was examined with a plane-plane Fabry-Perot interferometer and was found to have a single longitudinal mode at the same frequency as the seed-laser, with an M_x^2 = 1.3 and M_y^2 = 1.2. We further investigated the system with the PA pumping turned on and its gain changed by repositioning the 12.7 mm cylindrical lens to another fixed position so that the diode spot-size was increased within the $Nd:YVO_4$ crystal. The

second figure, figure 4(b), shows the output power of ~8 W with the PA operating at a SSSP gain of around 5. The M^2 of the beam in both directions remained unchanged. The last figure, figure 4(c), shows the spatial profile of the output beam when the SSSP gain of the PA was increased to ~10 (output power of ~11.4 W). The M^2 of this beam increased slightly in the horizontal direction to give $M_x^2 = 1.4$ but remained unchanged in the vertical direction with a $M_y^2 = 1.2$. This increase in the horizontal direction is due, partly, to an increasing misalignment between the two interfering beams with the FWM gain region caused by small displacements of the seed input beam upon passing through the pumped PA. The resonator, however, was still operating in a PC mode, shown by the fact that a severe-phase distortion (HF etched glass slide) could be placed into the resonator (at the position shown in figure 1) and still produce the same spatial profile output.

Modelling

Numerical modelling of such a PCO has already been studied extensively and reported in [9]. In this paper, Crofts *et al* modelled the gain saturation FWM and applied boundary conditions appropriate for an adaptive resonator. In this analysis we will look at a single transmission grating only as the reflection grating analysis is a simple extension of the theory presented here. The steady-state coupled equations derived for a transmission gain grating are [9]:

$$+\frac{dA_1}{dz} = \gamma_\tau A_1 + \kappa_\tau A_3 \tag{1a}$$

$$-\frac{dA_2}{dz} = \gamma_\tau A_2 + \kappa_\tau^* A_4 \tag{1b}$$

$$+\frac{dA_3}{dz} = \gamma_\tau A_3 + \kappa_\tau^* A_1 \tag{1c}$$

$$-\frac{dA_4}{dz} = \gamma_\tau A_4 + \kappa_\tau A_2 \tag{1d}$$

Where γ_τ and κ_τ are the self and diffractive coupling coefficients, respectively, and are defined in [9]. This model can be further developed to incorporate a PA in the output arm of the cavity by modifying the boundary conditions used (see figure 5) to give:

$$A_1(0) = A_+(L) \tag{1e}$$

$$A_3(0) = t_+ A_1(L) \tag{1f}$$

$$A_2(L) = t_- A_4(0) \tag{1g}$$

$$A_4(L) = 0 \tag{1h}$$

$$Aoutput = A_-(0) \tag{1i}$$

where *Aoutput* is the output field amplitude of the entire PCO-PA system. $A_+(L)$ and $A_-(0)$ are the single-pass output field amplitudes from the power-amplifier in the forward and backward directions respectively (see figure 5) and can be obtained by solving the following coupled equations using a numerical shooting routine:

$$\frac{dA_+}{dz} = \frac{g_0 A_+}{1+\left(\frac{|A_+|^2+|A_-|^2}{|A_{sat}|^2}\right)}$$
$$\frac{dA_-}{dz} = \frac{-g_0 A_-}{1+\left(\frac{|A_+|^2+|A_-|^2}{|A_{sat}|^2}\right)} \qquad \text{(1j)}$$

with the boundary conditions:

$$A_+(0) = \textit{seed input}$$
$$A_-(L) = A_2(0) = \textit{output from FWM} \qquad \text{(1k)}$$

where g_0 is the SSSP amplitude gain coefficient of the PA. Figure 6 shows the PCO-PA output intensity as a function of seed-laser input intensity (all normalised to saturation intensity, I_{sat}, of Nd:YVO_4 = 830 W cm^{-2}) for amplifier amplitude gain length products g_0L = 0, 0.8 and 1.2 corresponding to SSSP gains (G_0=exp($2g_0$L)) in the PA of 1, 5 and 10 respectively. The FWM-amplifier in all three cases has an $\alpha_0 L$ product of 4.15 (where α_0 is the amplitude gain coefficient of the FWM-amplifier) corresponding to an intensity gain of ~4000. As g_0 is increased the peak output intensity from the resonator also increases and occurs for a lower value of seed input intensity, a consequence of the fact that the seed laser passes through the PA before becoming the input to the PCO.

The model shows that by increasing the gain of the PA the PC output rises accordingly. Crofts *et al* [9] made the theoretical observation that adding a further PA inside the PCO loop would increase the PC output power. When the total gain of the loop was set to a constant value the highest output was obtained when all the available loop gain was concentrated in the FWM amplifier. In this paper, however, the amplifier is external to the loop where the high power PC output from the PCO experiences higher power extraction through the PA. This is in contrast to the situation analysed in [9] where the low power intracavity flux of the PCO produced low power extraction in the PA. In this model, with an external PA, the total loop gain-length coefficient is set to $\alpha_0 L + g_0 L = 5$. Figure 7 shows the PCO-PA output against the seed laser input for a selection of ratios of $\alpha_0 L$ and $g_0 L$. It can be seen from the graph that although the gain of the FWM amplifier decreases, the total PC output intensity initially increases due to the compensating increase in the gain of the PA. As the FWM amplifier gain is reduced further and the PA gain is increased the output from the system starts to fall due to the gain of the FWM being so low so as to give a very weak output. Further decreasing the FWM gain causes the PCO to fail to reach oscillation threshold and so no output is obtained. From this we can see that the distribution of gain between the FWM amplifier and the PA has some optimum value around which the output from the PCO-PA system starts to fall. Operation of the PCO-PA system around this optimum point will still produce a PC output (assuming the PCO has enough gain to reach threshold) but with reduced efficiency.

Conclusion

In conclusion, we have demonstrated that a phase-conjugate adaptive resonator can be power-scaled with the addition of a PA in the output arm of the phase-conjugating cavity, whilst still correcting for severe phase-aberrations in the resonator. The interactions taking place in the system have been successfully modelled and allow us to now further optimise the power-scaling of the PCO-PA by varying the distribution of the gain between the FWM amplifier and the PA.

Acknowledgements.

We would like to acknowledge the financial support of the Engineering and Physical Sciences Research Council (EPSRC) under grant numbers GR/R01545 and GR/N01552/01. We also gratefully acknowledge Spectron lasers, UK for their funding of JMH under a CASE award.

References

1. Spectra-Physics Inc., http://www.splasers.com/products/pdfs/Monsoon_ds.pdf
2. Y.F.Chen, L.J.Lee, T.M.Huang, C.L.Wang, Optics Comm., **163**, 198, (1999).
3. S.Guy, C.L.Bonner, D.P.Shepherd, D.C.Hanna, A.C.Tropper, B.Ferrand, IEEE J. Quantum Electron., **34**, 900, (1998).
4. A.Giesen, H.Hugel, A.Voss, K.Wittig, U.Brauch, H.Opower, Appl. Phys. B,**58**, 365, (1994).
5. M.Trew, G.J.Crofts, M.J.Damzen, J.Hendricks, S.Mailis, D.P.Shepherd, A.C.Tropper, R.W.Eason, Opt. Lett., **25**, 1346, (2000).
6. S.Mailis, J.Hendricks, D.P.Shepherd, A.C.Tropper, N.Moore, R.W.Eason, G.J.Crofts, M.Trew, M.J.Damzen, Opt. Lett., **24**, 972, (1999).
7. JDSU CASIX Inc., P.O. Box 1103, Fuzhou, Fujian 350014, China (http://www.casix.com).
8. J.E.Bernard, A.J.Alcock, Opt. Lett., **18**, 968, (1993).
9. G.J.Crofts, M.J.Damzen, Optics Comm., **175**, 397, (2000).

Figure Captions.

Fig 1. Schematic of the adaptive laser resonator with a power amplifier in the output arm of the loop. A phase-distorter can be placed in the resonator loop at the position shown to investigate the phase conjugation ability of the system.

Fig 2. The phase-conjugate output power of the combined adaptive resonator and power-amplifier as a function of seed-laser input power for various amplifier gains. Maximum PC output increases with amplifier gain and occurs for smaller values of input seed power.

Fig 3. Intracavity flux curves of the clockwise resonator beam (measured at point A in figure 1) as a function of seed input power.

Fig 4. The spatial profiles of the phase-conjugate output for (a) $\alpha_0 L = 4.15,\ g_0 L = 0$ (b) $\alpha_0 L = 4.15,\ g_0 L = 0.8$ and (c) $\alpha_0 L = 4.15,\ g_0 L = 1.2$.

Fig 5. Schematic showing the boundary conditions used to incorporate the power-amplifier into the adaptive resonator model [9].

Fig 6. The modelled power input-output curves of the combined adaptive-resonator power-amplifier system for a fixed $\alpha_0 L = 4.15$ and various power amplifier gains of $g_0 L = 0$ (squares), $g_0 L = 0.8$ (diamonds) and $g_0 L = 1.2$ (triangles).

Fig 7. The modelled power input-output curves of the combined adaptive-resonator power-amplifier. The total gain of the two amplifiers is held constant and is distributed between them in various ratios.

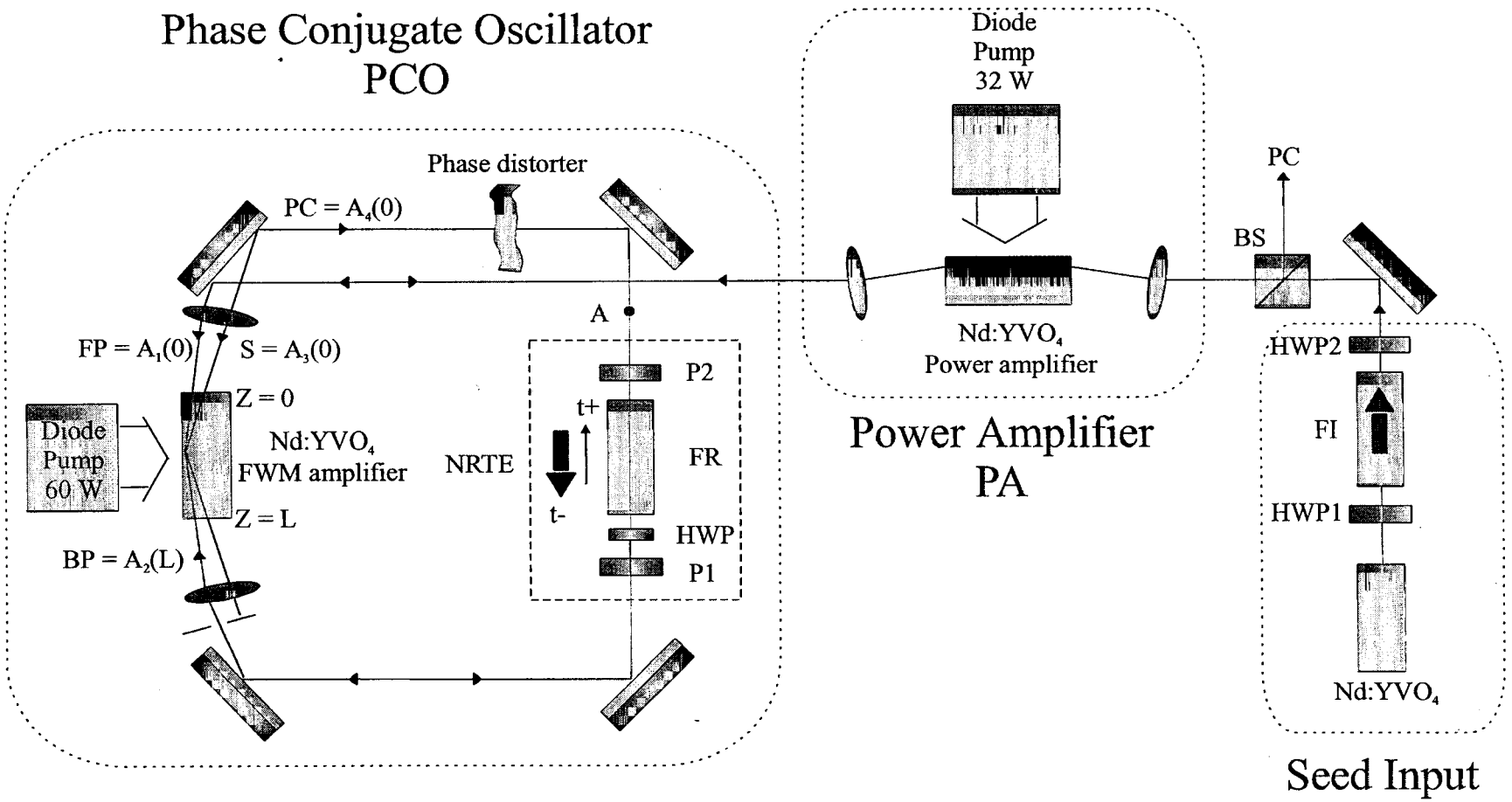
Phase Conjugate Oscillator
PCO
Phase distorter
PC = A4(0)
FP = A1(0)
S = A3(0)
Z = 0
Diode
Pump
60 W
Nd:YVO4
FWM amplifier
Z = L
BP = A2(L)
NRTE
A
P2
t+
FR
t-
HWP
P1
Diode
Pump
32 W
Nd:YVO4
Power amplifier
Power Amplifier
PA
PC
BS
HWP2
FI
HWP1
Nd:YVO4
Seed Input

Figure 1

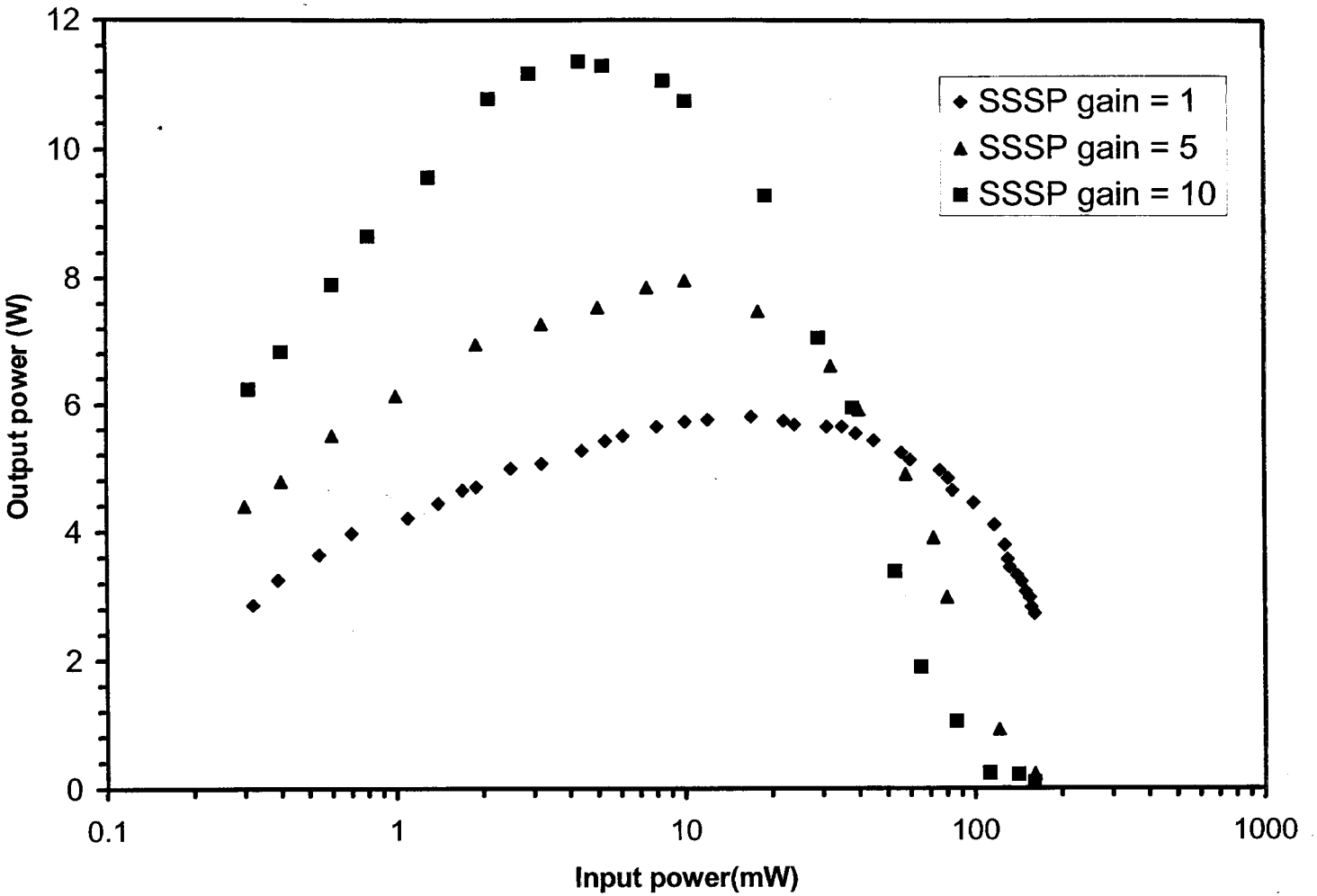
12
10
8
6
4
2
0
Output power (W)
0.1
1
10
100
1000
Input power(mW)
SSSP gain = 1
SSSP gain = 5
SSSP gain = 10

Figure 2

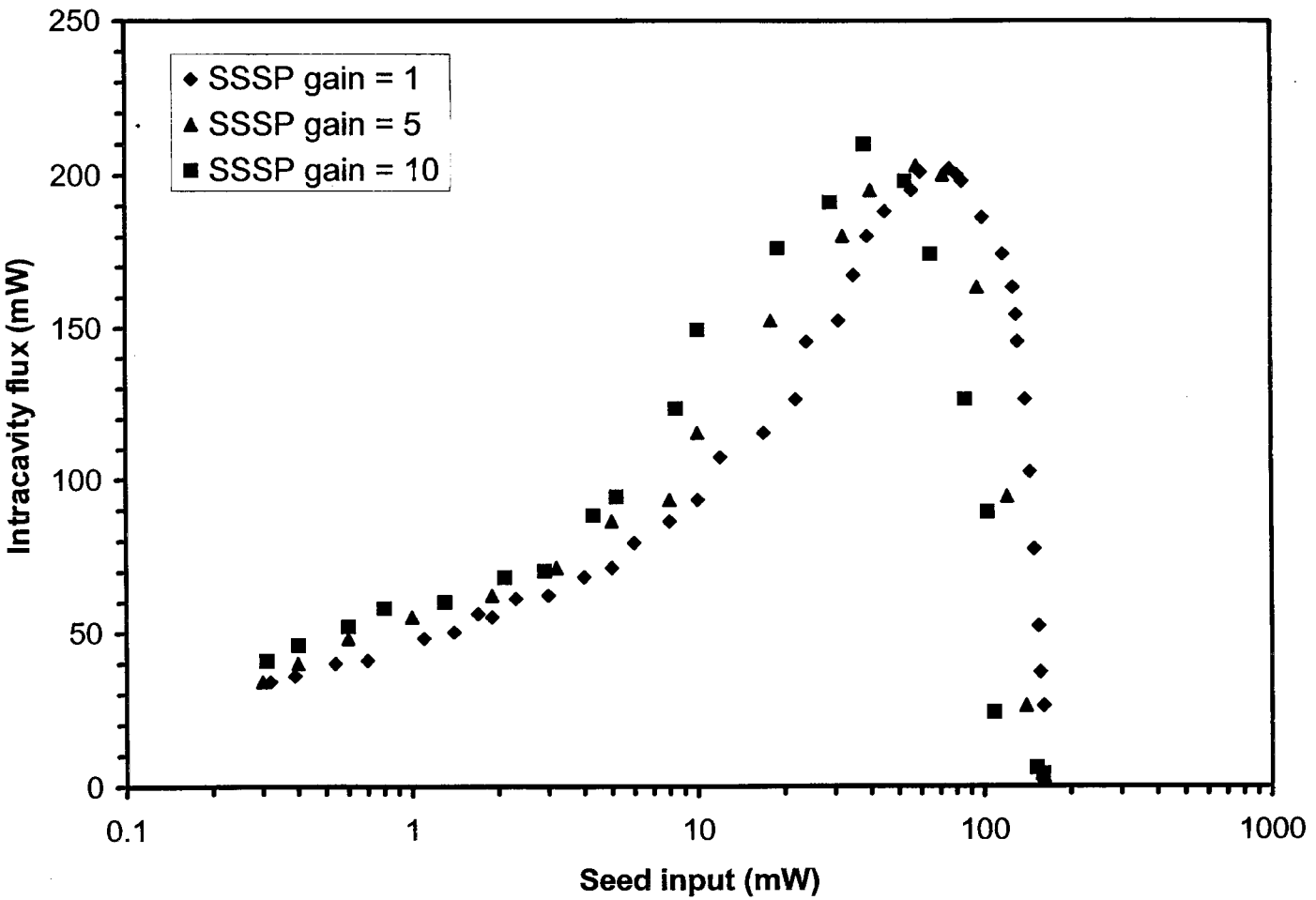
SSSP gain = 1
SSSP gain = 5
SSSP gain = 10
Intracavity flux (mW)
Seed input (mW)
250
200
150
100
50
0
0.1
1
10
100
1000

Figure 3

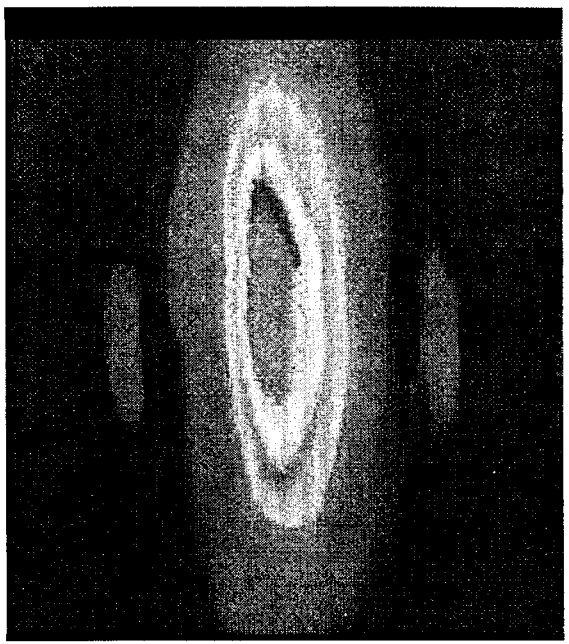

4(a)

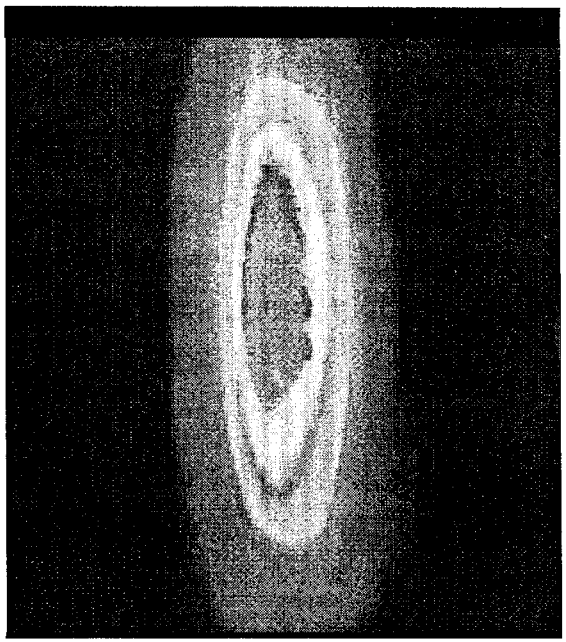

4(b)

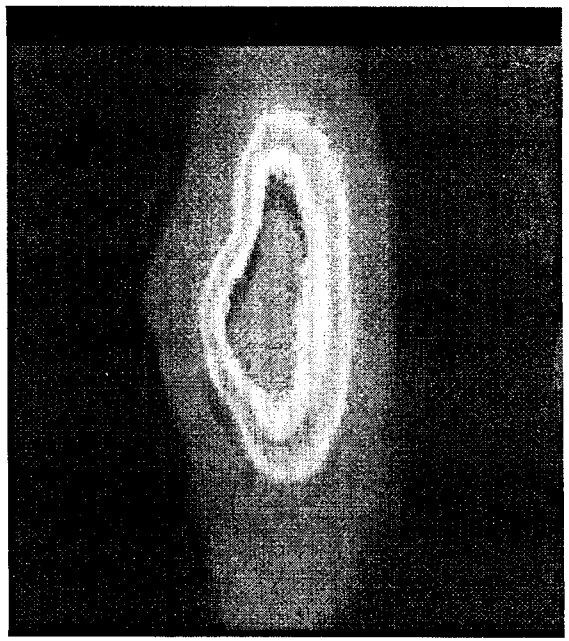

4(c)

Figure 4

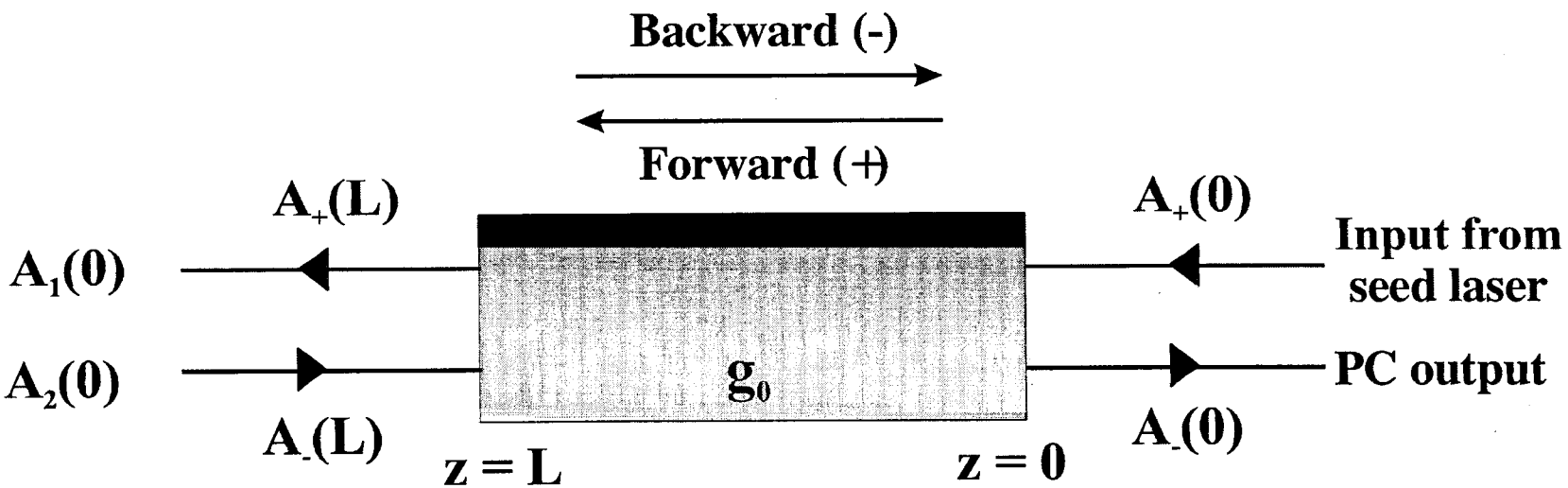
Backward (-)
Forward (+)
$A_+(L)$
$A_+(0)$
$A_1(0)$
Input from seed laser
$A_2(0)$
g_0
PC output
$A_-(L)$
$A_-(0)$
z = L
z = 0

Figure 5

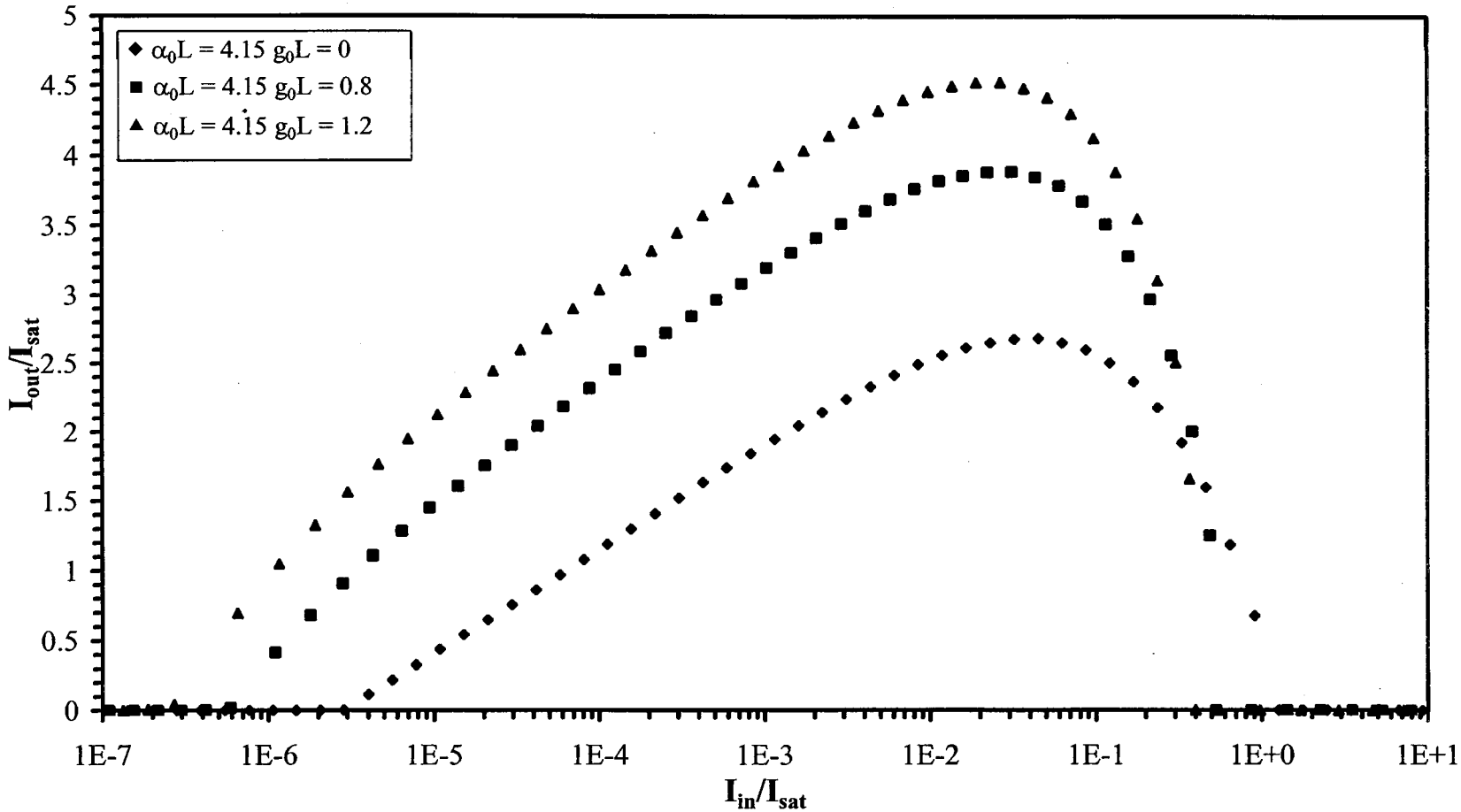
◆ $\alpha_0 L = 4.15$ $g_0 L = 0$
■ $\alpha_0 L = 4.15$ $g_0 L = 0.8$
▲ $\alpha_0 L = 4.15$ $g_0 L = 1.2$
I_{out}/I_{sat}
I_{in}/I_{sat}
0
0.5
1
1.5
2
2.5
3
3.5
4
4.5
5
1E-7
1E-6
1E-5
1E-4
1E-3
1E-2
1E-1
1E+0
1E+1

Figure 6

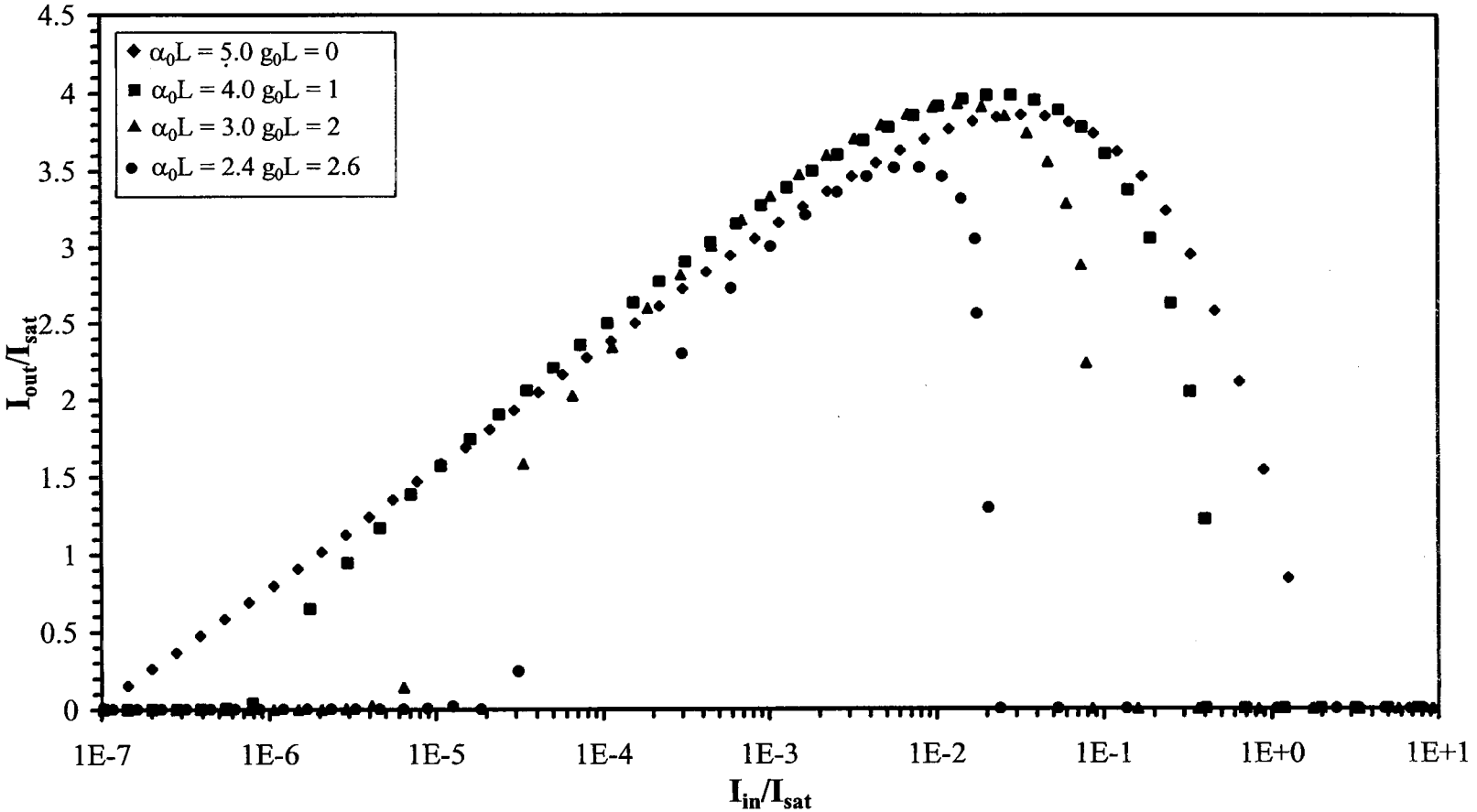
◆ $\alpha_0 L = 5.0$ $g_0 L = 0$
■ $\alpha_0 L = 4.0$ $g_0 L = 1$
▲ $\alpha_0 L = 3.0$ $g_0 L = 2$
● $\alpha_0 L = 2.4$ $g_0 L = 2.6$
4.5
4
3.5
3
2.5
2
1.5
1
0.5
0
I_{out}/I_{sat}
1E-7
1E-6
1E-5
1E-4
1E-3
1E-2
1E-1
1E+0
1E+1
I_{in}/I_{sat}

Figure 7